Spontaneous Pattern Formation in an Effectively One-Dimensional Dielectric-Barrier Discharge System

J. Guikema, N. Miller, J. Niehof, M. Klein, and M. Walhout*

Department of Physics and Astronomy, Calvin College, Grand Rapids, Michigan 49546

(Received 13 April 2000; revised manuscript received 12 July 2000)

In a dielectric-barrier discharge between diametrically opposite sides of a narrow tube, discharge filaments stabilize at regular intervals along the tube's length. Three types of periodic patterns are observed, as is a disordered state in which filaments fire at apparently random positions and times. Time-resolved current measurements indicate that for each spatial pattern, a particular number of discharge stages occur during the voltage half-cycle. A preliminary model of the pattern-formation dynamics is described, motivating further work on time-resolved imaging and investigations of surface charge distributions.

PACS numbers: 47.54.+r, 05.45.Ac, 05.65.+b, 52.80.Tn

Dielectric-barrier discharges (DBD's) comprise a specific class of high-voltage, ac, gaseous discharges that typically operate in the near-atmospheric pressure range. Their defining feature is the presence of dielectric layers that make it impossible for charges generated in the gas to reach the conducting electrodes. With each half-cycle of the driving oscillation, breakdown leads to the formation of narrow discharge filaments that deposit charge on the dielectric surfaces. Accumulating charge reduces the voltage drop across each filament until a discharge can no longer be sustained, whereupon the filament is extinguished. Since the low charge mobility on the dielectric limits the lateral region over which the gap voltage is diminished, parallel filaments can form in close proximity to one another. A typical filament may be roughly 0.1 mm in diameter and last only about 10 ns.

The DBD's unique combination of nonequilibrium and quasicontinuous behavior has motivated a range of applications and fundamental studies. Its use in industrial ozone reactors has generated interest in optimizing specific chemical processes and prompted studies of different gas mixtures, electrical characteristics, and geometries [1–3]. Related work has focused on maximizing the ultraviolet radiation produced by excimer molecules in DBD's [4–6]. Models of single-filament dynamics have accounted for two- and three-body reactions involving electrons, ions, neutral atoms, and photons [7–9]. On another research front, it has been seen that the transverse distribution of discharge filaments in 2D, parallel-plate DBD's can take the form of stable, large-scale patterns reminiscent of those associated with magnetic domains or Rayleigh-Bénard convection [10–13]. These patterns have been modeled using methods that apply generally to pattern formation in nonlinear dynamical systems [14–16]. Thus, the dynamical interactions *between* filaments, as well as the chemical and electronic interactions *within* filaments, have proven interesting.

In this paper we present observations of periodic filament patterns and apparent spatiotemporal chaos in an effectively one-dimensional (1D) DBD configuration—that is, a DBD in which filaments are constrained to a line perpendicular to the applied electric field. Our discharge cell is a 30-cm-long, cylindrical glass tube with a 2.0-mm inner diameter and a 7.5-mm outer diameter. Stripes of silver paint, 3 mm wide, are applied on diametrically opposite portions of the outer surface. Sparking around the outside of the cell is avoided by means of a jacket of insulating transformer oil, which is contained within a second glass tube. A sinusoidal ac voltage is applied across the cell electrodes, which extend through rubber seals at opposite ends of the outer tube (see Fig. 1). The 1-to-20-kHz signal is derived from a function generator, fed through a 2-kW audio amplifier, and then stepped up with a high-voltage transformer. The present investigations of He-Ar mixtures make use of a simple mixing manifold, into which each gas flows continuously at a rate indicated by a flow meter. Adjustable balance valves on either side of the tube provide precise control over the rate and direction of mixed gas flow through the discharge region. We normally set these valves to cancel the opposing flows in the tube.

Owing to the curvature of the inner surface of the cell, our DBD is tightly constrained in one lateral dimension and

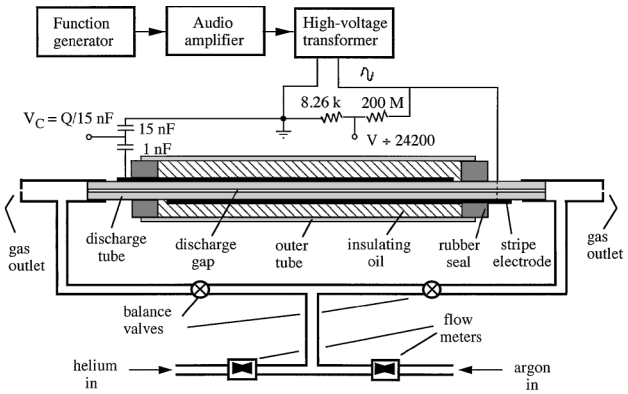

FIG. 1. Schematic of experimental setup. A video camera (not shown) is used to capture close-up images of the discharge gap, where filaments form periodic patterns along the tube length.

supports purely 1D patterns along the tube's length. With larger inner diameters, we have seen some wandering of filaments in the dimension perpendicular to the cylindrical axis. However, having chosen a tube with an inner radius smaller than the characteristic size of a discharge footprint (i.e., patch of deposited surface charge), we observe a suppression of filaments not localized to the plane containing the electrode axes. Thus, we call this an effectively 1D system and expect to model it using 1D charge and current distributions integrated over the azimuthal dimension of the cylindrical gap. We expect this simplification to contribute to a unified understanding of individual filament behavior and the dynamics of spatiotemporal pattern formation.

A video camera and frame grabber allow us to record pictures of the discharge and to analyze the digitized frames. The spacing measurements presented below were obtained with a resolution of 115 ± 2 pixels/cm along the tube axis. The average spacing (λ) is calculated for each image as the distance between the centers of widely separated (nonadjacent) filaments, divided by the number of intervening filament spaces. The mean deviation from this large-scale average is one of two dominant contributions to our uncertainty in λ. The other arises from gas mixture uncertainties. All experiments presented here utilize a gas mixture with a He:Ar number-density ratio of 2:1 at a pressure of 760 ± 20 Torr. We estimate that an uncertainty of about 2% in λ is introduced by possible short-term mixture and pressure fluctuations. This value is added in quadrature to the average local spacing deviation in order to generate the statistical uncertainty represented by our error bars for λ.

Another diagnostic involves the circuit shown in Fig. 1. We monitor the voltage across the tube [$V = V_0 \sin(2\pi\nu t)$] and the voltage across a series capacitor (V_C), the latter being proportional to the charge (Q) stored on the electrodes. To maintain proper tuning of the circuit, we make sure that, for V_0 below breakdown, a V_C-vs-V oscilloscope trace (or QV plot) falls along a line with slope proportional to the capacitance of the discharge tube. With a discharge running, the jumps in Q corresponding to filamentary discharges cause the trace to take on an open, sliverlike shape. We will have occasion to examine the temporal distribution of these jumps more closely in the following discussion.

Figure 2 shows a sequence of ten horizontal images of the discharge tube, which is driven in this case at a frequency $\nu = 16$ kHz. Each image corresponds to a different V_0 and is integrated over four voltage cycles. Stationary (repeating) filaments are seen as bright, vertical stripes that widen at the tube wall. The patterns formed by these filaments are of three distinct kinds, which we give the following names: type A patterns appearing in the general range of $450 < V_0 < 610$ V and exhibiting narrow filaments with relatively wide separations; type B patterns ($610 < V_0 < 940$ V), with narrow filaments separated by roughly half of the typical type A spacing; and type C patterns ($980 < V_0 < 1200$ V), characterized by alternating bright, wide filaments and dim, narrow filaments.

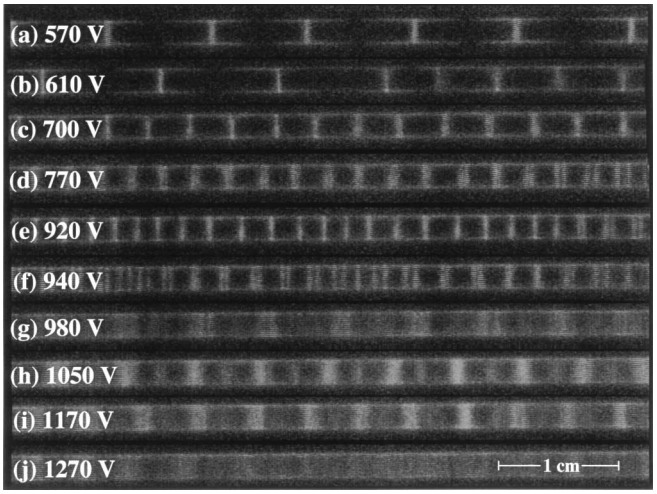

FIG. 2. Ten images of the DBD for $\nu = 16$ kHz and various driving amplitudes (V_0 indicated for each image). Images (a) and (b) show patterns of type A, with (b) also revealing a stable pattern front that can occasionally be seen for $V_0 = V_{A\to B}$. Images (c)–(e) display type B patterns; (e) and (f) exhibit a long-wavelength bunching effect that can sometimes be found in the type B pattern as the system approaches a second instability. For voltages between those indicated in (f) and (g), filaments strike at random times and places. Images (g)–(i) show type C patterns, which are most distinct when V_0 is near the center of the stability window. Image (j) shows the lack of filament pattern (chaos) that is characteristic of higher voltage amplitudes.

For V_0 between 940 and 980 V or above 1250 V, filaments strike at apparently random locations—behavior that may indicate spatiotemporal chaos. Such a characterization must be qualified by time-resolved data such as that shown in Fig. 3. In plots 3(a)–3(c), sharp steps in V_C reveal that discharge types A, B, and C are associated, respectively, with the presence of one, two, and three distinct discharge stages in each voltage half-cycle. However, for conditions producing spatial disorder on time scales down to the half-cycle, all but one or two of the V_C steps disappear and discharges occur over an extended interval [plot 3(d)]. The disappearance of V_C steps indicates that an abrupt increase in temporal disorder accompanies the transition to spatial disorder.

Three additional features in Fig. 2 are noteworthy. First, image 2(b) shows A and B type patterns separated by a "front" that can be made stationary if V_0 is set precisely. Second, a long-wavelength bunching effect is observed in images 2(e) and 2(f), possibly suggesting a zero-wave-number instability setting in when V_0 is on the verge of pushing the system into disorder. Third, in order to acquire images of stationary patterns, we sometimes find it necessary to adjust the gas-flow balance valves slightly, with the effect of stopping an otherwise moving pattern. The flow required to balance the pattern motion generally

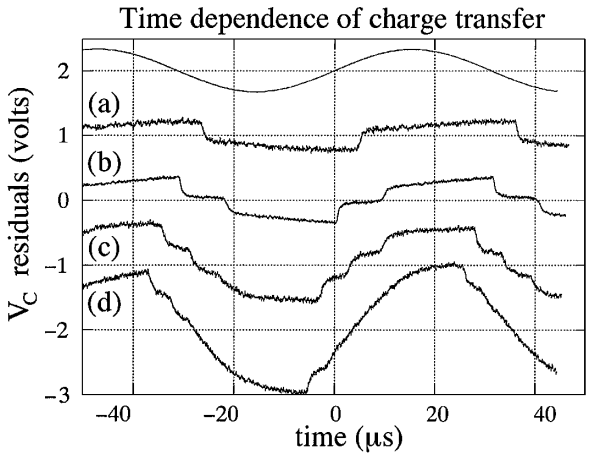

FIG. 3. Digital oscilloscope traces of V_C reveal the timing of individual discharge stages, as well as the relative amount of the charge transferred across the tube during each stage. Each of the labeled traces shows V_C data after subtraction of an appropriately scaled sinusoid that is in phase with the 16-kHz driving oscillation (indicated at top). Trace (a), with a single discharge stage per half-cycle, corresponds to a type A pattern. Trace (b) exhibits a pair of discharge stages and corresponds to a type B pattern. In trace (c), we see that one of the three discharge stages corresponding to a type C pattern actually strikes in the direction opposing the applied field, indicating that the surface-charge field has become dominant. Trace (d), which corresponds to a spatially disordered state, shows an extended period of filament formation replacing the otherwise distinct discharge stages. Each trace is actually centered at zero volts, with offsets being introduced for the sake of presentation.

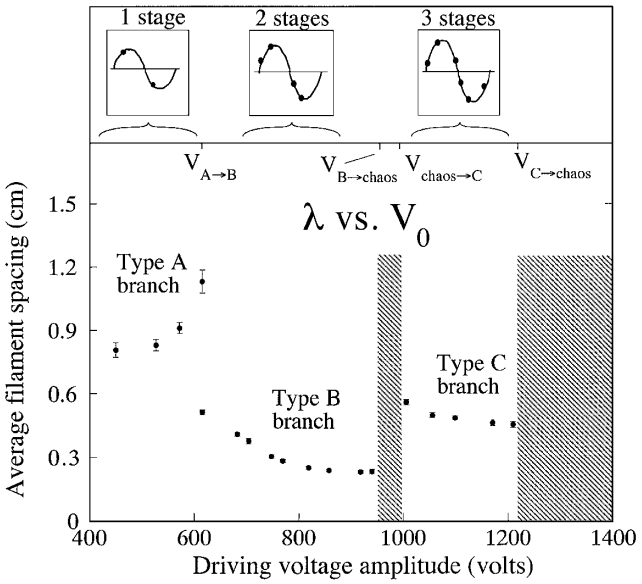

FIG. 4. Bottom: Measured average filament spacings (λ) vs driving amplitude (V_0). Each of the branches corresponds to one of the three pattern types observed. Shaded regions indicate voltage ranges for which the filament distribution appears spatially and temporally disordered. The data are for increasing V_0; if V_0 decreases, slight hysteresis is seen in the transition voltages. Top: Three schematic representations of a single cycle of V_C. Each dark spot shown on the voltage trace indicates the position of a jump caused by a discharge stage. Patterns of type A, B, and C correspond, respectively, to one, two, and three distinct discharge stages per voltage half-cycle.

increases with V_0, but we have not completed a systematic study of traveling pattern modes. Such rich behavior invites further analysis of the dynamics and stability of the system.

In Fig. 4 we plot λ vs V_0 for the images in Fig. 2 (plus additional points taken during the same run). Each of the three branches shown in the plot corresponds to one of the three patterns. We have obtained data similar to that of Fig. 4 for various frequencies between 4 and 20 kHz, with qualitatively similar results. While experiments are reproducible in detail in the course of several hours, we find that the transition voltages $V_{A\to B}$, $V_{B\to\text{chaos}}$, $V_{\text{chaos}\to C}$, and $V_{C\to\text{chaos}}$ can vary by up to a factor of 2 over several days, perhaps as a result of low-level contamination or changes in ambient pressure. However, the A, B, and C branches are always seen to fall in the same ranges of λ whatever the applied frequency. And all our data are consistent with the rough proportionality $V_{B\to\text{chaos}} = (1.4 \pm 0.2)V_{A\to B}$.

We now sketch the beginnings of a model that we are developing to explain the observed patterns, addressing first a general mechanism that contributes to the long-term stability of any DBD filament pattern. Assuming filaments to form and transfer charge as discussed elsewhere [1], we note that a single, isolated filament will tend to remain stationary because the surface charge it deposits during one half-cycle produces a field enhancement when the voltage changes sign. That is, the localized site of charge deposited in one half-cycle is a probable site of filamentation in the next half-cycle. In the context of pattern formation, this "memory" effect helps ensure that each filament stays in nearly the same place, so that patterns remain stationary once they are formed.

Along with reasons for filament stabilization, we wish to find reasons for uniform filament spacing. We consider the distribution of charge along the dielectric surface and the alteration it produces in the profile of the electric field in the gas. For convenience, we make the simplifying (strictly incorrect) assumption that positive and negative charge footprints have similar spatial distributions, of which we consider only longitudinal variations. We also assume that nearly identical filaments form along the full length of the tube, and we describe the tube ends as having ramped boundary conditions with a characteristic length scale of about 1 cm. This scenario leaves room for significant longitudinal slippage of the endmost filaments and is consistent with our observations. Within this model, we expect uniform filament spacing to arise from a balancing of two competing effects: On one hand, a sufficiently high electric field tends to initiate filament formation; on the other, charge deposition partially cancels the field (until the applied voltage changes sign).

Type A patterns appear if, after a single discharge stage, the fringe fields from adjacent footprints hold the local field below breakdown, even as the voltage reaches V_0. This condition gives rise to a maximum filament spacing for type A patterns that depends on V_0 and on the footprint charge distribution. A minimum filament spacing must also exist, since every footprint field suppresses nearby filamentation. We expect the footprint size itself to be a characteristic measure of the minimum spacing. The reproducibility of type A patterns suggests that the minimum and maximum spacing values are in fact equal, so that the filament spacing is unique over most of the V_0 range. Conceivably, this would be the situation in our model if the footprint charge could be distributed appropriately.

Our model also affords some understanding of type B patterns. As V_0 is increased along the A branch, the first discharge stage appears more and more in advance of the driving voltage maximum, and the electric field increases significantly after the first stage is completed. When V_0 reaches $V_{A\rightarrow B}$, breakdown can occur in the spaces between the first-stage footprints, where the rising field is attenuated least. This onset of a second discharge stage initiates the transition to a type B pattern, during which the density of filaments is roughly doubled. Correspondingly, for reasons that are not yet clear, the footprint size appears to be roughly halved. Given the low time resolution of our camera, we are unable to determine experimentally whether the type B pattern is an interleaving of two patterns that appear during consecutive discharge stages or whether in fact all of its filaments fire twice during each half-cycle. Our model leads us to argue for the former scenario, but without time-resolved images, we remain unsure which is the case.

Except for very general notions regarding the possible interactions of charge footprints with the applied field and with each other, we have little understanding of the detailed shape of the A and B branches in Fig. 4. Neither do we have much insight as to how type C patterns are stabilized. Our model would seem to allow a pattern of alternating wide and narrow filaments to occur if the appropriate footprint charge distributions could be established. However, we have yet to develop a quantitative understanding of footprint profiles for any of the three pattern types. In future experiments, we will therefore focus on obtaining footprint measurements from images like those in Fig. 2. We also plan to develop time-resolved imaging techniques that will allow us to associate spatial filament structures with particular discharge stages. With such information in hand, we will likely be able to develop and test a quantitative version of our 1D model. We thus hope to advance the understanding of DBD patterns generally, possibly to an extent that will allow patterns to be used to diagnose specific plasma conditions in applications requiring control over chemical or radiative processes.

This work has been supported by Research Corporation (Award No. CC4251), the National Science Foundation (NSF 9876679), and Calvin College. For the loan of equipment items, M. W. thanks colleagues in the Physics Laboratory at NIST, Gaithersburg, MD.

*Author to whom correspondence should be addressed.

[1] B. Eliasson and U. Kogelschatz, IEEE Trans. Plasma Sci. **19**, 309 (1991).
[2] B. Eliasson and U. Kogelschatz, IEEE Trans. Plasma Sci. **19**, 1063 (1991).
[3] D. Braun, U. Kuchler, and G. Pietsch, J. Phys. D **24**, 564 (1991).
[4] B. Gellert and U. Kogelschatz, Appl. Phys. B **52**, 14 (1991).
[5] K. Stockwald and M. Neiger, Contrib. Plasma Phys. **35**, 15 (1995).
[6] J-Y. Zhang and I. W. Boyd, J. Appl. Phys. **80**, 633 (1996).
[7] S. Yagi and M. Tanaka, J. Phys. D **12**, 1509 (1979).
[8] B. Eliasson, M. Hirth, and U. Kogelschatz, J. Phys. D **20**, 1421 (1987).
[9] W. Sun, B. Pashaie, S. Dhali, and F. J. Honea, J. Appl. Phys. **79**, 3438 (1996).
[10] D. G. Boyers and W. A. Tiller, Appl. Phys. Lett. **41**, 28 (1982).
[11] E. Ammelt, D. Schweng, and H.-G. Purwins, Phys. Lett. A **179**, 348 (1993).
[12] Y. A. Astrov, E. Ammelt, and H.-G. Purwins, Phys. Rev. Lett. **78**, 3129 (1997).
[13] Y. A. Astrov, I. Muller, E. Ammelt, and H.-G. Purwins, Phys. Rev. Lett. **80**, 5341 (1998).
[14] M. C. Cross and P. C. Hohenberg, Rev. Mod. Phys. **65**, 851 (1993).
[15] C. P. Schenk, M. Or-Guil, M. Bode, and H.-G. Purwins, Phys. Rev. Lett. **78**, 3781 (1997).
[16] I. Brauer, C. Punset, H.-G. Purwins, and J. P. Boeuf, J. Appl. Phys. **85**, 7569 (1999).